JGP Journal of General Physiology

TUTORIAL

A primer on resolving the nanoscale structure of the plasma membrane with light and electron microscopy

Justin W. Taraska

The plasma membrane separates a cell from its external environment. All materials and signals that enter or leave the cell must cross this hydrophobic barrier. Understanding the architecture and dynamics of the plasma membrane has been a central focus of general cellular physiology. Both light and electron microscopy have been fundamental in this endeavor and have been used to reveal the dense, complex, and dynamic nanoscale landscape of the plasma membrane. Here, I review classic and recent developments in the methods used to image and study the structure of the plasma membrane, particularly light, electron, and correlative microscopies. I will discuss their history and use for mapping the plasma membrane and focus on how these tools have provided a structural framework for understanding the membrane at the scale of molecules. Finally, I will describe how these studies provide a roadmap for determining the nanoscale architecture of other organelles and entire cells in order to bridge the gap between cellular form and function.

Introduction

All cellular life is surrounded by a thin bilayer made of phospholipids (Robertson, 1981, 2018). This hydrophobic barrier compartmentalizes and concentrates the complex chemical reactions of the cell. It is a vital feature of life. Evidence that this structure was made out of a thin sheet of hydrophobic molecules (a membrane) was obtained ∼100 yr ago with electrical and chemical measurements of cells (Fricke, 1925; Fricke and Morse, 1925; Gorter and Grendel, 1925; Danielli, 1935). Fast forward 20 yr and the first images of cells and tissues at the nanoscale were made with the electron microscope (Porter et al., 1945; Satir, 1997). These early studies revealed that a simple molecular bilayer is the primary cellular barrier. Thus, all transport and communication between cells and their environment must involve the movement of signals and materials across this membrane. Decades of study have led to a deep understanding of the structure of the plasma membrane and its roles in biology and physiology (Singer and Nicolson, 1972; Singer, 1974; Robertson, 1981, 2018; Kusumi et al., 2012). Microscopy has been central to revealing these foundations.

Here, I will review several key classic and recent developments in light and EM that have been used to map the structure of the plasma membrane and study its biology. In this context, I will discuss the physical and practical aspects of these methods, what was learned from their use, and their future development and extension to understand the general physiology of the plasma membrane and other organelles. Throughout the review, I will emphasize how key features of the plasma membrane have allowed it to be a testbed for new microscopies. This is due to two primary features of the plasma membrane: (1) It is the most exterior cellular organelle and thus more easily probed with new measurement tools, and (2) it is, for all practical purposes, a 2-D system that makes wide-field visualization, analysis, and modeling simpler than that for 3-D systems. Thus, the history of plasma membrane imaging can provide a roadmap for how future work can be designed and leveraged to gain a comprehensive global map of the molecular structure of entire cells, tissues, and organisms (Taraska, 2015).

EM

The earliest views of the plasma membrane were obtained through the combined development of the electron microscope and electron-dense cellular stains and fixatives (Hall et al., 1945; Porter et al., 1945; Watson, 1958a,b; Moberg, 1995). Why are stains and fixatives important for EM? For an electron microscope to visualize a sample, the electrons passing through or scattering off the sample must interact with the material. Electrons interact only weakly with carbon-based matter, and thus,

Biochemistry and Biophysics Center, National Heart, Lung, and Blood Institute, National Institutes of Health, Bethesda, MD.

Correspondence to Justin W. Taraska: justin.taraska@nih.gov.

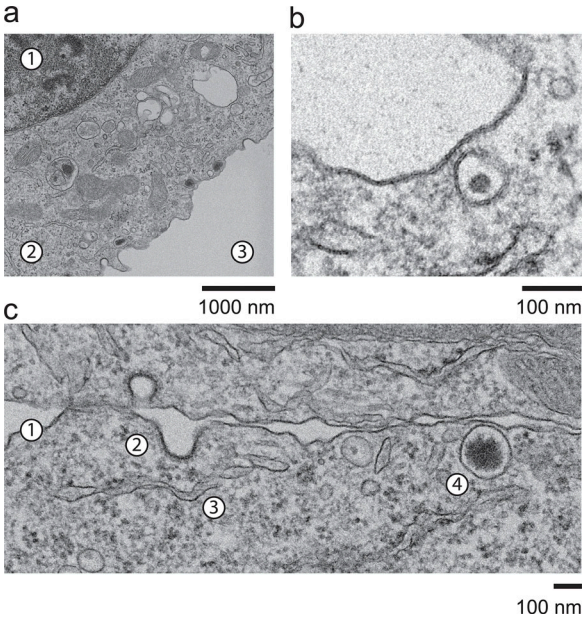

Figure 1. **Thin-section transmission electron micrographs of cells. (a)** Cultured rat Ins-1 cell showing the (1) nucleus, (2) cytoplasm, and (3) extracellular space around the cell. **(b)** Zoomed view of a PC12 cell plasma membrane showing the stained bilayer and a single dense-core vesicle. **(c)** Magnified section of two Ins-1 cells showing the (1) plasma membrane, (2) clathrin-coated pit, (3) internal membranes, and (4) dense core vesicle. Cells were prepared and imaged using methods similar to those described previously (Graffe et al., 2015).

most biological objects have very little inherent contrast in an electron microscope. However, heavy metals, with their densely packed nuclei, interact strongly with passing electrons. Thus, early physiologists seeking contrast in EM at achievable electron voltages began to use heavy metal salts such as lead, osmium, and uranium as stains and fixatives for biological samples (Watson, 1958a,b). A cellular structure that reacts particularly well with stains is the phospholipid bilayer (Fig. 1). When combined with plastic embedding techniques and ultramicrotome cutting to trim thin sections of cells, these methods revealed in never-before-seen detail that cells are surrounded by an ultrathin bilayer of phospholipids (Porter and Blum, 1953; Glauert et al., 1956; Glauert and Glauert, 1958; Watson, 1958a,b). These early EM images clearly showed the complexity and topography of the membrane enwrapping cells. Thin finger-like processes, many pits and invaginations, and associated vesicles were evident, suggesting a dynamic membrane system at the cell's edge (Fig. 1; Roth and Porter, 1964).

Recent developments have revolutionized thin-section EM. Previously, it was difficult to obtain extensive 3-D data of cells with serial-section EM techniques, because they were done mostly by the trained hand of an experienced microtomist (Harris et al., 2006). New automated microtome-enabled scanning electron microscopes, tape-based section capture machines, and focused ion beam milling instruments now allow samples to be sectioned and imaged repeatedly with a voxel size approaching 5 nm across entire cells (Kizilyaprak et al., 2018). Thus, the complete 3-D structure of many external and internal membrane systems and even entire cells and tissues are now being tracked (Briggman et al., 2011; Briggman and Bock, 2012; Helmstaedter et al., 2013; Glancy et al., 2015). These images are dense with information about the topography of the plasma membrane and how it relates to other cellular structures. As these datasets become developed and full 3-D models of cells are built, a detailed understanding of the cell's complex membrane architecture will be gained. This is currently a major knowledge gap in general cellular physiology.

Although thin-section EM provides resolution at the nanometer scale, it does not show the dense protein components of the cell as clearly as it does the membrane (Fig. 1). This is due to two general reasons. First, many EM stains interact better with phospholipids and darkly stain the membrane. Second, the dense packing and continuity of the membrane produces one extended resolvable object. Long continuous objects are easier to distinguish in an image; as an example, one notices a jet's contrail in the sky more than a single small puffy cloud. Thus, thin-section EM techniques were (and are) best used to reveal the topography of extended membranes, but not the particulate proteinaceous components of those membranes (e.g., cytoskeleton, membrane proteins, and membrane coats). For example, endocytic invaginations, including clathrin-coated pits or caveolae, can be identified in cross sections of the cell's plasma membrane (Fig. 1; Roth and Porter, 1964; Heuser and Reese, 1981), yet much of the protein machinery associated with these membrane organelles are generally difficult to see.

Early in the development of EM, the making of metal replicas was rapidly adopted (Williams and Wyckoff, 1945a,b). Metal replicas are made by coating samples with a thin layer of electron-dense metal such as gold or platinum. This produces a metal "replica" of the sample's surface (Fig. 2). In fact, the biological material is generally dissolved away, leaving behind just the metal coating. Replicas are usually further coated with a thin layer of carbon to stabilize the samples. These replicas are resistant to damage by electrons, provide high contrast in EM and are stable for decades. Thus, metal/carbon–coated samples can be repeatedly imaged with high contrast and high resolution with transmission or scanning EM (Heuser, 2014). With replicas, even single isolated proteins were seen >70 yr ago (Williams and Wyckoff, 1945a,b). Platinum replica EM is still the gold standard for visualizing the dense protein-based structure of the plasma membrane and even deep into the cell with freeze-fracture techniques (Meier and Beckmann, 2018). Other exotic metals or carbon itself might produce even better resolution (Cabezas and Risco, 2006; Krystofiak et al., 2019). Furthermore, when metals are evaporated on the sample from one side, the metal shadow cast by the height of the sample produces a contrast effect that makes the replicas appear 3-D (Williams and Wyckoff, 1946). In a sense, samples appear to have stage lighting (Fig. 2). This effect has been used to study at the shape and size of biomolecules in EM (Williams and Wyckoff, 1945a,b).

Because of these advantages, metal replica EM has been instrumental in showing the nanoscale structure of the plasma membrane with all its associated filaments, organelles, and proteins (Fig. 2; Heuser, 2014). To access the inside of the cell with replicas, however, additional treatments must

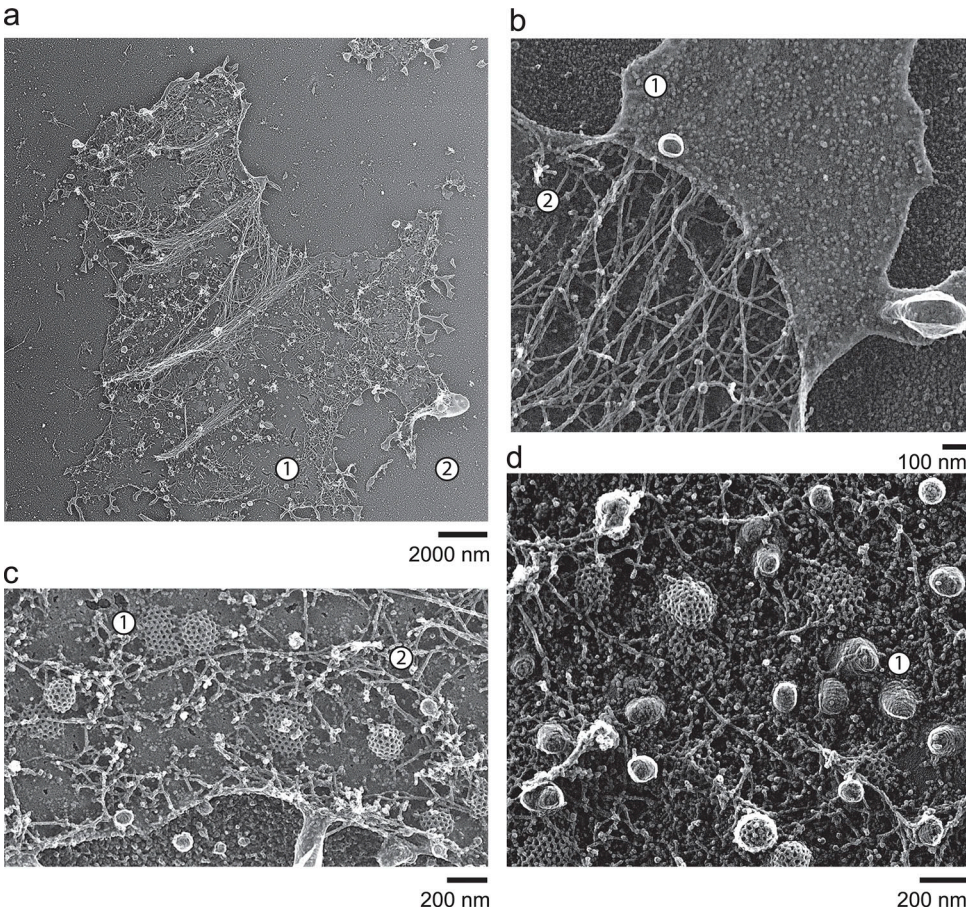

Figure 2. **Platinum replica electron micrographs of unroofed cells. (a)** An entire HeLa cell plasma membrane showing (1) the inner surface of the plasma membrane and (2) outside the cell. **(b)** Zoomed view of an unroofed HeLa cell showing the (1) outer surface of the plasma membrane and (2) inner surface of the plasma membrane. **(c)** Zoomed view of a HeLa cell plasma membrane showing (1) clathrin-coated sites and (2) the actin cortex. **(d)** Image of a U-87 glioblastoma cell plasma membrane with numerous (1) caveolae. Cells were prepared and imaged using methods similar to those described previously (Sochacki et al., 2012, 2017).

be employed. One of the primary methods used to expose the cell's interior for metal coating is freeze fracture (Meier and Beckmann, 2018). In freeze fracture, frozen cells are hit with a cold knife to "fracture" apart continuous pieces of cell. Because membranes are a weak point, the cell can split or fracture between planes of the membrane, exposing this surface, which can be coated with metal. Specifically, four different surfaces of the cell's membrane system can be exposed for metal coating and imaging (E surface, extracellular membrane side; E face, internal side of the extracellular bilayer; P surface, intracellular side of the membrane; and P face, internal side of the bilayer from the cytoplasmic side; Meier and Beckmann, 2018). This is unique to freeze-fracture EM and allowed for the membrane to be viewed in ways that other methods could not show. Similar to other samples, these replicas can be imaged with transmission or scanning EM to produce an image.

While less commonly practiced today, the structures revealed in early freeze-fracture images are mysterious and evocative. For example, some embedded membrane proteins are clearly exposed. Thus, clustering, packing, ordering, and interactions of membrane proteins could be studied in their native context. Smaller protein complexes, along with larger structures such as the nuclear pore and gap junctions, could be resolved at the nanoscale and across hundreds of square microns of space (Heuser and Salpeter, 1979). One specific example is the study of the neuromuscular junction of a motor terminal (Heuser and Reese, 1981). In these classic images, aligned rows of membrane embedded particles could be seen to organize alongside exocytic fusion sites in the synaptic terminal (Heuser and Reese, 1981). Vesicles appeared to fuse near these "tracks" of proteins. Thus, the fusion machinery and calcium channels that trigger exocytosis were hypothesized to organize into nanoscale domains in the synapse. The molecular identities of these structures are still an area of study.

Another common approach to access the inside of the cell is a technique called "unroofing" (Clarke et al., 1975; Mazia et al., 1975; Vacquier, 1975; Avery et al., 2000; Heuser, 2000). Here, cells that are attached to a substrate are opened with a sheering force either by sonication or a jet of liquid. This treatment removes the top of the cell and organelles and cytoplasm not associated with the adherent plasma membrane. Specifically, the nucleus, Golgi, and ER are mostly washed away. What remains is the exposed inner adherent plasma membrane, associated proteins, and organelles (Fig. 2). If the sample is fixed during

unroofing, it can then be frozen or dried and coated with metal in a vacuum to create a replica. These samples have been used to produce some of the highest resolution and strikingly beautiful images of molecular complexes at the cell's plasma membrane (Heuser, 2000; Fig. 2).

What one notices immediately with a metal replica transmission electron microscope image of an unroofed cell is the unbelievable complexity and density of the inner plasma membrane (Fig. 2). For example, the outer membrane looks essentially homogenous, containing a fairly uniform coating of small bumps, domes, and pits (Fig. 2). The inner membrane, however, is dense with honeycomb clathrin-coated structures in many shapes and sizes, both flat and curved caveolae with their watermelon-striped coat, and numerous distinct filament systems that are densely packed, branched, and woven together (Fig. 2). Only a limited number of small cleared nanoscale patches of empty membrane can be seen without noticeable molecular detail. Even these patches of plasma membranes, however, commonly contain clustered or single particles likely corresponding to membrane-embedded proteins like receptors or ion channels. Many unknown or unidentified structures are visible in these images; their names and functions a mystery. These include large smooth membrane invaginations and vesicles, uniquely shaped smaller vesicles that form teardrops or crescents, complex bundled filaments, cross-links, and clusters of proteins. A future understanding of these unidentified objects will require linking a protein or activity to these specific physical structures (Taraska, 2015).

In the process of making a replica, the metal coats the cell evenly, revealing the shape of all the material that is present in the sample. Because the objects are visible, but the individual molecular species are hard to identify, replicas have been primarily used to study the structure of organelles and complexes that can be clearly identified by their shapes alone. For example, because clathrin creates a fine lattice of regular hexagons and pentagons, the clathrin coat has been a favorite topic of study for platinum replica EM (Fig. 2; Heuser, 1980, 1989; Heuser and Keen, 1988; Collins et al., 2011; Sochacki et al., 2012; Vassilopoulos et al., 2014). The same is true for caveolae, endosomal sorting complexes required for transport (ESCRTs), and the structure of the membrane-associated cytoskeleton (Heuser and Kirschner, 1980; Heuser, 1986; Rothberg et al., 1992; Morone et al., 2006; Hanson et al., 2008). The actin cortex and its association with the membrane can be studied across entire cells at the nanoscale with specialized stabilization and extraction methods (Ishikawa et al., 1982; Tsukita et al., 1982; Svitkina and Borisy, 1999; Morone et al., 2006; Yang and Svitkina, 2019). Here, the branching patterns, filament lengths, bundling, and local distributions and associations of filaments with membranes have been extensively investigated with replicas in neurons and other cultured cells (Svitkina et al., 1986; Svitkina and Borisy, 1999; Morone et al., 2006; Yang and Svitkina, 2011, 2019). However, the same limitations to all of EM apply to replicas. Namely, the image is a single snapshot of one moment, one time, in the cell. Specifically, to prepare samples, they must be fixed or frozen and stabilized for imaging. Thus, time-dependent changes in these structures must be inferred from their relative numbers and assumptions about their kinetics and pathways of growth. To obtain time-domain information, other methods must be used.

Over the last decade, EM has experienced a sea change (Milne et al., 2013; Cheng, 2018; Ognjenović et al., 2019). With the development of direct-electron detector cameras and new image processing tools to video, enhance, select, and average low-contrast EM images, the field has made major leaps forward in resolution and contrast (Henderson, 2015). Many of these developments have been aimed at determining the structure of single molecules by particle averaging (Cheng, 2018). But parallel and equally exciting developments have occurred for 3-D imaging and reconstruction of cryo-frozen cells known as cryo-electron tomography (cryo-ET; Gan and Jensen, 2012; Villa et al., 2013; Beck and Baumeister, 2016; Oikonomou and Jensen, 2017). The major advantage of cryo-ET over replicas and other 3-D methods is that cells can be imaged close to their native states. Specifically, because cells can be rapidly frozen, crystalline ice cannot form, and the cell is incased in vitreous frozen water. In these experiments, no contrast agents are added and the cell can be imaged at very low temperatures. With the addition of phase plates, these images can be striking (Glaeser, 2013). Similar to platinum-replica EM, these samples can resolve the protein and membrane structures that make up the cell. Combined with subtomogram averaging (e.g. selection, alignment, and averaging of similar areas of a structure within an image), these methods allow for the determination of the dense "native-like" structure of the membrane and surrounding proteins at atomic resolution (Schur et al., 2013; Wan and Briggs, 2016; Bykov et al., 2017). However, the lack of additional stains means that all contrast must be obtained from the cellular material itself, which can be dim (Milne et al., 2013). Thus, alternative contrast-generating mechanisms, including phase contrast or averaging, need to be used to study these samples. The samples are also very delicate, and the EM beam can rapidly heat and damage the sample, making imaging tricky. Finally, similar to platinum-replica EM, because all carbon-based objects in the sample produce contrast, these images can be dense and difficult to segment. Currently, there is no easy way to tag and identity all of the components that make up these images. Thus, other protein-specific labeling methods need to be developed in the future. Nonetheless, cryo-EM and cryo-ET have recently produced amazing images of close-to living cells in their native states. A few notable examples are the structure of the proteasome in neurons, the intraflagellar transport motor complex in cilia, chloroplasts, nuclear membranes, microtubules, and the COP coat (Engel et al., 2015; Mahamid et al., 2016; Bykov et al., 2017; Jordan et al., 2018; Kovtun et al., 2018). Future improvements in the fitting of heterogenous shapes into EM densities will likely be key to allowing for the native search for protein structures in dense samples (Nickell et al., 2006; Villa and Lasker, 2014; Xu et al., 2019).

While EM produces beautiful images and much development has been aimed at improving the hardware and protocols for physical imaging, methods designed at quantitative measurement and analysis of those images is equally important for biological discovery (Myers, 2012). Image analysis tools, however,

have in some ways lagged behind. To this day, a great deal of image processing and analysis in the biological and medical sciences is done with manual identification and segmentation of objects from micrographs. The availability of many open-source, free, powerful, and community-centered image processing tools, however, is fundamentally increasing the speed and distribution of automated, semiautomated, and quantitative image analysis pipelines (Walter et al., 2010; de Chaumont et al., 2012; Eliceiri et al., 2012; Schindelin et al., 2012; Mastronarde and Held, 2017; Schorb et al., 2019; Xu et al., 2019). The first and possibly most pressing analysis challenge for EM is the segmentation of images into their relevant measurable objects. Segmentation can be incredibly difficult where objects of interest reside in a sea of other objects of equal contrast with similar shapes and densities (Briggman and Bock, 2012). Thus, extracting specific objects is a challenge. However, recent improvements in machine learning or other more classical image processing methods are rapidly advancing the field of image segmentation (Moen et al., 2019). Thus, a future where images can be mined and analyzed at scale is hopefully near at hand. One fast-moving area is the automated segmentation and processing of single-particle cryo-EM data to solve the atomic structure of purified proteins (Henderson, 2015). Similar gains in segmenting, measuring, and extracting data from complex images of cells and tissues would provide massive benefits to our understanding of the structure of the plasma membrane and other organelles across cells and tissues.

Light microscopy

EM in all its forms is well suited to resolving the nanoscale structure of the plasma membrane. The membrane is, however, a dynamic space made of specific molecules with specific functions. Organelles grow and dissolve, filaments extend and branch, and different proteins rapidly move through this complex environment over the course of milliseconds to minutes to hours. Proteins interact in heterogeneous, transient, and dynamic complexes. Understanding these properties (the dynamic protein-specific functional architecture of the membrane) is key to understanding the design and regulation of the system as a whole. Fluorescence microscopy, which can label and track chosen biomolecules, is well suited to follow identified proteins in living cells (Taraska and Zagotta, 2010; Crivat and Taraska, 2012). Clearly, there are thousands of papers and hundreds of years of study that have used light to track the physical structure of the membrane. Indeed, the first description of the cell as a compartmentalized membrane-bound object was made with a simple light microscope >350 yr ago (Hooke, 1665). A deep understanding of the proteins associated with the plasma membrane and their dynamics has been obtained with bright-field, polarization, and fluorescence microscopy. Classic optical fluorescence microscopy, however, whether confocal illumination or epifluorescence illumination, is limited in resolution to the optical diffraction limit (Huang et al., 2009). Resolution is the distance at which two structures can be distinguished as separate. This limit generally hovers around 200 nm in the transverse plane and ≤500 nm in the axial plane when a high-numerical-aperture microscope objective is used (Sigal et al., 2018). This is larger than the size of many key biological

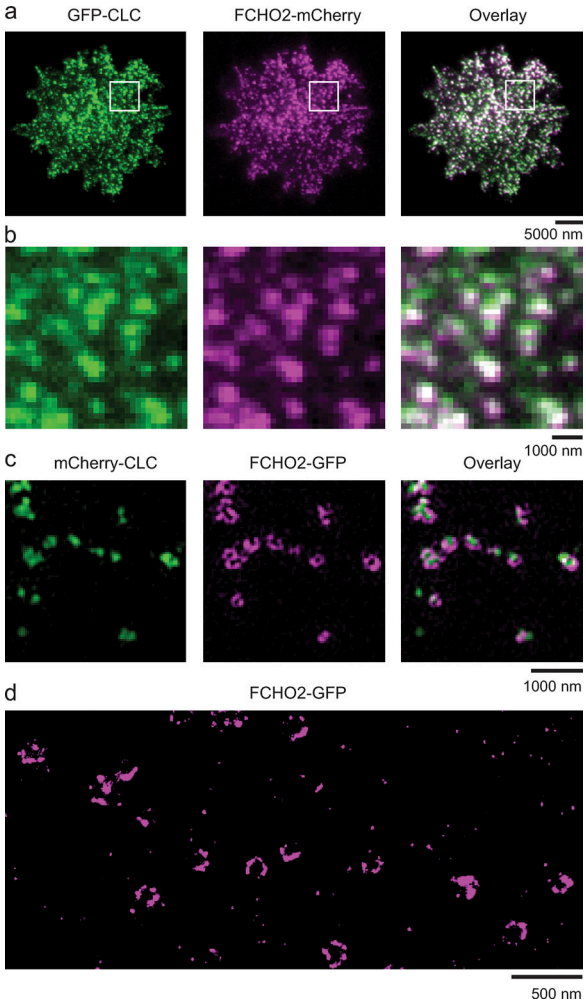

Figure 3. **Fluorescence micrographs of the plasma membrane. (a)** TIRF image of an intact live PC12 cell expressing clathrin light chain (CLC; green) and FCHO2 (red) and the overlay image (Larson et al., 2014). **(b)** Zoomed images from white boxes in panel a. **(c)** TIRF-SIM image of intact HeLa cell expressing clathrin (green) and FCHO2 (red) and the overlay image (Sochacki et al., 2017). **(d)** Superresolution direct stochastic optical reconstruction microscopy (dSTORM) localization image of Alexa Fluor 647/nanobody–labeled FCHO2 expressed in an unroofed HeLa cell (Sochacki et al., 2017).

objects on the plasma membrane. For example, clathrin-coated pits are ∼150 nm in diameter and caveolae are ∼90 nm. Thus, other methods needed to be developed to image at a scale that matches the structure of objects on the membrane.

One of the first fluorescence methods developed to study the real-time dynamics of the plasma membrane was TIRF, also known as evanescent field microscopy (Fig. 3; Axelrod, 1981, 2013; Steyer and Almers, 2001). TIRF, while producing a conventional resolution in the transverse plane, breaks the diffraction limit in the axial dimension to illuminate cells with a subwavelength (∼100 nm deep) field of excitation light (Axelrod, 1981). This field illuminates the membrane vicinity but leaves the rest of the cell dark, producing a high-contrast, low-background image of the attached plasma membrane (Fig. 3; Axelrod, 2013). With ultrahigh-numerical-aperture objectives, this field can be as shallow as 50 nm, the size of some of the

smallest organelles at the plasma membrane such as synaptic vesicles (Zenisek et al., 2000).

TIRF has exploded in use over the last 20 yr (Steyer and Almers, 2001; Mattheyses et al., 2010). Its ease of application, commercial development, and superior image contrast have made it the primary imaging mode for tracking fluorescently labeled structures at the plasma membrane. Its ability to uniquely image single molecules has also enabled the development of localization-based superresolution methods (discussed below). Furthermore, the development of new, brighter, multicolor, genetic, organic, and semisynthetic fusion tags has allowed for the tracking of multiple different organelles and proteins (Wysocki and Lavis, 2011; Crivat and Taraska, 2012; Specht et al., 2017). Dozens of groundbreaking papers over the years have revealed the local dynamics of plasma membrane structures with TIRF at millisecond time resolutions in living cells. These have included the tracking of single vesicles fusing with the plasma membrane, endocytic vesicles retrieving cargo, single-receptor dynamics, and adhesion structure dynamics, to name a few (Steyer and Almers, 2001; Mattheyses et al., 2010). In these studies, the complexity of the proteins that assemble and regulate these biological systems is large. Tracking how and when they arrive, how they assemble together, and what they do is the next step in understanding how they work in health and malfunction in disease.

Unique electromagnetic features of evanescent fields have been harnessed to characterize the behavior of molecules and organelles at the plasma membrane. For example, by varying the angle of the excitation beam, the evanescent field can be made shallow or deep across a set of images. Comparing these images allows for the 3-D position of labeled organelles to be mapped (Olveczky et al., 1997; Rohrbach, 2000). These "multiangle" TIRF experiments have the potential to track the dynamics of organelles and even single molecules at the nanometer scale in live cells.

A second modification of TIRF that has been used to monitor the structure of the plasma membrane is varying the polarization of the excitation beam (Sund et al., 1999). When a polarized laser is used to generate an evanescent field, the resulting excitation field is polarized (Sund et al., 1999). This polarization selectively excites the absorption dipoles of dyes that are aligned with the direction of polarization. Thus, the orientation of those fluorophores can be mapped by tracking the resulting emission generated by two oppositely polarized fields (Zenisek et al., 2002; Taraska and Almers, 2004). Recently, this method has gained traction to image the behavior of exocytic and endocytic vesicles at the plasma membrane (Anantharam et al., 2010, 2011; Passmore et al., 2014; Scott et al., 2018). For example, the real-time shape of exocytic vesicles has been monitored when dense core vesicles fuse with the membrane in chromaffin cells and when clathrin-coated pits curve (Anantharam et al., 2010, 2011; Scott et al., 2018). These studies have provided direct insights into how membranes bend during membrane fusion and fission events, showing the dynamic heterogeneity of these plasma membrane/organelle systems in live cells.

TIRF provides a major advantage over classical fluorescence methods: the ability to clearly image single molecules (Funatsu et al., 1995). TIRF can do this primarily due to its extreme signal-to-noise advantage. With modern scientific cameras, a fluorophore resting in the evanescent field at low density appears as a bright diffraction-limited spot (Thompson et al., 2002; Yildiz et al., 2003). This fact, paired with the development of photoactivatable or "blinking" fluorophores, has ushered in the development of superresolution localization-based imaging methods (Patterson and Lippincott-Schwartz, 2002; Patterson et al., 2010). The major leap that occurred in the development of these methods was the realization that if a single molecule could be imaged, and if it was certain that this was a single molecule, then a Gaussian function could be fit to the point-spread function of the single fluorescent spot to estimate the center of this emitting molecule with nanometer precision (Betzig, 1995; Thompson et al., 2002; Yildiz et al., 2003). This idea was used to track single molecules moving in nanometer steps (Yildiz et al., 2003, 2004). When paired with photoactivatable molecules that could be switched on and off with light or with chemicals, these methods allowed for the production of images of entire cells with fluorescent localization precisions well below the traditional diffraction limit (Fig. 3; Patterson and Lippincott-Schwartz, 2002; Betzig et al., 2006; Hess et al., 2006; Rust et al., 2006).

Because most superresolution localization-based methods rely on TIRF to achieve the incredibly high contrast necessary to image single molecules, many of the experimental studies using superresolution light imaging have focused on studying the organization or dynamics of proteins at the plasma membrane (Ji et al., 2008; Huang et al., 2010; Patterson et al., 2010; Hauser et al., 2017; Stone et al., 2017; Sigal et al., 2018). There are now many studies that have used superresolution methods to explore the nanoscale structure of proteins at the plasma membrane (Stone et al., 2017; Sigal et al., 2018; Jacobson et al., 2019). Examples include the structure of the cytoskeleton in neurons, receptor dynamics at the plasma membrane, and the organization of individual organelles. In each of these cases, the complex architecture of the proteins is being revealed (Ji et al., 2008; Sigal et al., 2018). These studies have been done both in live and fixed cells, and new combinations of superresolution methods are being used to explore the structure and behavior of proteins faster and for longer periods of time (Winter and Shroff, 2014; Wu and Shroff, 2018).

Another modification of TIRF that has gained prominence over the last decade is the merger of structured illumination microscopy (SIM) and evanescent field illumination (Fig. 3; Gustafsson, 2000; Kner et al., 2009; Guo et al., 2018). This method, called TIRF-SIM, is able to break the diffraction limit by using patterned illumination that can be reconstructed to produce an image with a resolution that is twice as good as that of a conventional TIRF microscope (Gustafsson, 2000; Kner et al., 2009). As a result, objects like filaments and vesicles that have structures below the diffraction limit can be tracked and studied over time in multiple colors. Thus, both structure and dynamics can be observed.

Finally, other point-scanning fluorescent methods like stimulated-emission depletion and minimal emission fluxes (MINFLUX) imaging have been able to break the diffraction

limit to image single events at the plasma membrane in live cells (Hell and Wichmann, 1994; Egner and Hell, 2005; Balzarotti et al., 2017). Recent examples include imaging the flow of lipids into and out of vesicles fusing with the membrane in chromaffin cells and the shape, size, and dynamics of fusion pores (Zhao et al., 2016; Shin et al., 2018). Again, the dynamics of single types of proteins can be imaged over time in live cells below the diffraction limit.

What has been discovered with superresolution fluorescent imaging of the membrane (Sigal et al., 2018; Jacobson et al., 2019)? One major advantage of fluorescence over EM is its ability to produce distinctive and quantitative signals from a single species in the dense environment of intact cells. For example, a protein can be tagged with a dye and imaged with high contrast, leaving the rest of the cell in the dark (Crivat and Taraska, 2012). Thus, specific patterns or structures built by individual proteins can be more easily segmented and quantitatively measured than with EM (Walter et al., 2010; Eliceiri et al., 2012; Myers, 2012; Coltharp et al., 2014; Caicedo et al., 2017). Recent developments and distributions of new image processing tools and pipelines are accelerating biological discovery with these types of statistical and quantitative measurement tools. The combined use of high-throughput, machine learning, and mathematical analysis of images will further speed this process (Walter et al., 2010; Eliceiri et al., 2012; Levet et al., 2015; Beghin et al., 2017; Caicedo et al., 2017; Weigert et al., 2018). With these analysis methods, previously unseen periodic rings of actin were seen in the axons of neurons (Xu et al., 2013; Leterrier et al., 2017). Likewise, the trafficking and diffusion patterns of receptors were observed on the surface of cells and the distribution of protein on organelles were observed with molecular resolution (Manley et al., 2008; Kanchanawong et al., 2010; Picco et al., 2015; Penn et al., 2017; Stone et al., 2017; Mund et al., 2018). What these studies have shown is that at the nanoscale, many processes have distinct structures that influence their behaviors (Kusumi et al., 2012). In essence, the design of the cell is built at the scale of molecules. Understanding the behavior of cells requires tools that can clearly identify and map this molecular design.

Correlative light and EM (CLEM)

What is missing in a fluorescent image? What is missing is the dense unlabeled components of the cell invisible to the fluorescent microscope: the dark material. The material surrounding the fluorophore, however, can be provided by other nonfluorescent imaging modalities (de Boer et al., 2015; Loussert Fonta and Humbel, 2015; Karreman et al., 2016; Hauser et al., 2017). These can include bright-field white light imaging, phase contrast, differential interference contrast, reflection interference contrast imaging, EM, and many other methods. The combination of more than one imaging modality to provide context and added structural or molecular information to a sample is commonly called correlative microscopy and, in the specific case of light and EM, CLEM (Fig. 4).

Investigations into the structure of the membrane are a place where CLEM has shone (de Boer et al., 2015; Loussert Fonta and Humbel, 2015; Hauser et al., 2017; Kopek et al., 2017; Russell et al., 2017). This is due to several features of CLEM. First, for EM, the membrane is one of the most salient features. Specifically, in thin-section EM, the plasma and internal membranes are darkly stained with high contrast, making them clearly visible at the nanometer scale across the entire cell (Fig. 1). The protein material is, however, less evident. This allows for the structure of the membrane and its topography to be studied (Watanabe et al., 2011; Kopek et al., 2013). By combining the location of proteins with fluorescence and the structure of the membrane with EM, a more complete view of the cell is obtained. The weakness is that while the bilayer is visible in EM, most other cellular objects other than DNA and ribosomes are not darkly stained and thus not clearly visible in thin-section EM.

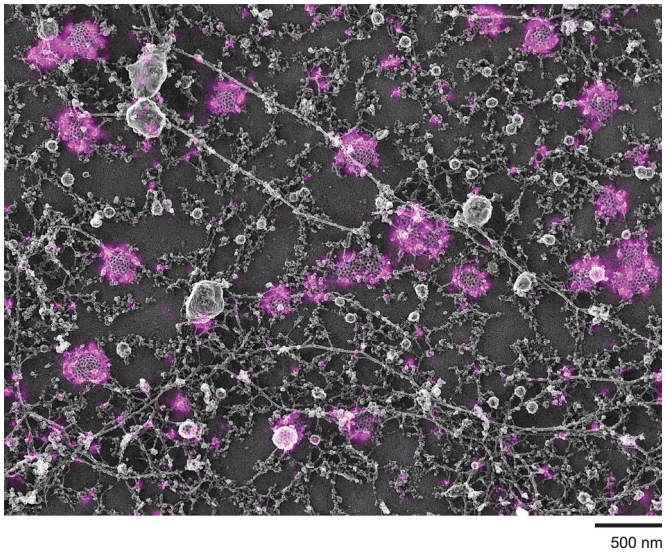

Figure 4. **Correlative micrograph of the plasma membrane.** Correlative superresolution light and platinum replica EM image of Alexa Fluor 647/nanobody–labeled FCHO2 (magenta, fluorescence) and the inner plasma membrane (gray, transmission EM) in an unroofed HeLa cell (Sochacki et al., 2017).

In platinum replica EM, however, the complete dense structure of the cell is resolved at nanometer scale in a stable sample that is resistant to EM damage (Figs. 2 and 4; Sochacki et al., 2014). Thus, the combination of light and platinum replica EM has been particularly fruitful in studying the structure of the membrane and membrane-associated complexes (Sochacki et al., 2014; Sochacki and Taraska, 2017). This is mostly a result of the fact that the atomic coating of metal adheres to cellular material evenly, revealing the surface structure of all molecules associated with the membrane. As mentioned above, EM samples mostly lack information about the identity of the proteins that make up these structures. A few proteins that assemble as distinctive lattices including clathrin, cavins/caveolins, or ESCRT proteins are exceptions (Heuser, 1980; Rothberg et al., 1992; Hanson et al., 2008). However, unroofed samples that are useful for EM are also suitable for high-resolution fluorescence imaging. The thin membranes (<100 nm thick) with no cellular background make for ultrasharp fluorescence images. Here, individual proteins can be localized

at the nanoscale (Sochacki et al., 2014). Current technical limitations make it such that only one to three different proteins can reasonably be imaged in each sample, yet these images allow for the annotated landscape of the membrane to be mapped (Sochacki et al., 2017).

CLEM and EM methods are rapidly opening new ways of mapping the cellular landscape. Below, I will present several recent examples of CLEM being used to map the structure of molecular events at the plasma membrane. These studies focused on the structural dynamics of endocytosis in both yeast and mammalian cells. Here, the units of study are small, 100-nm endocytic vesicles that grow and form at the plasma membrane. These are below the diffraction limit for a conventional light microscope. Furthermore, these structures grow and curve in three dimensions. Thus, the use of CLEM to map the dynamic assembly of the coat and how the membrane curves and its relationship to the surrounding cellular architecture is key to understanding the system (Fig. 4). In this regard, endocytosis is a system that is excellent to explore with CLEM.

CLEM's power rests in combining the advantages of two complementary imaging modes. Light microscopy's advantages are the ability to measure the same event directly through time and space and the ability to label and identify specific proteins with ease. This allows for dynamic events to be sequenced and protein types to be tracked both temporally and spatially in a living cell. This is inherently difficult to do with EM, where the time domain has been notoriously hard to access and labeling, detection, and counting of specific proteins are challenging in dense EM samples. In a clever set of papers, a method for imaging thin cellular sections prepared for EM with epifluorescence in two colors was developed (Kukulski et al., 2011, 2012, 2016). Next, the authors relied on the fact that a set of proteins could be used in combination to specifically mark the stages of endocytosis in yeast. Thus, colocalizing spots in fluorescence were used to determine the location of endocytic vesicles at different stages of endocytosis. Thus, the curvature and shape of organelles at the plasma membrane could be measured with EM (Kukulski et al., 2012). Taken together, they were able to map the structural transitions that occur at the plasma membrane during single endocytic events, a spectacular achievement. Interestingly, the fluorescent imaging in this work was diffraction limited epifluorescence and far above the resolution needed to see the structure of each vesicle, yet the patches of fluorescence used to locate and identify the areas to image in EM were good enough to map them with specificity. Here, the power of combining fluorescence with the benefits of EM is clear. A later study used the same method to track the curvature of endocytic structure in mammalian cells (Avinoam et al., 2015). From these images, the authors propose a pathway for plasma membrane curvature during single clathrin-mediated endocytic events.

In diffraction limited CLEM (e.g., epifluorescence, confocal, TIRF microscopy) the proteins that are associated with subcellular structures cannot be mapped with nanoscale precision. This is where the combination of superresolution light and EM has become a powerful method (Chang et al., 2014; de Boer et al., 2015; Hauser et al., 2017; Kopek et al., 2017). Because the precision of superresolution light microscopy (8–50 nm and sometimes better) aligns well with the resolution of EM (1 nm or better), single fluorophore-labeled proteins can be overlaid directly on cellular ultrastructure. This has been done for thin-section, cryo-EM, and platinum replica EM using localization microscopy-based super resolution imaging (Hauser et al., 2017; Kopek et al., 2017).

Determining the structure of the clathrin coat has been a particularly fruitful system to explore with CLEM (Fig. 4; Sochacki et al., 2014, 2017). Here, clathrin is proposed to assemble as a local complex of adaptors, cargo, and clathrin triskelia. This nascent lattice grows, loads additional cargo, and curves (Sochacki and Taraska, 2019). The domed membrane vesicle continues to curve into a sphere when the mechanoenzyme dynamin is recruited, assembles as a polymer, and cuts the neck of the pit to form a sealed endocytic vesicle. Dozens of proteins regulate stages of this process at the nanoscale, but the nanoscale structure and assembly of all the factors was unknown (Haucke and Kozlov, 2018; Sochacki and Taraska, 2019).

Because superresolution is useful to map individual proteins at the nanoscale and platinum replica EM can show the location, shape, lattice pattern, and curvature of the clathrin coat, combining both methods has given a detailed view into the assembly of proteins around the growing lattice. These studies have shown that a set of proteins assemble exclusively at the rim of the clathrin coat to form a ring of proteins (Sochacki et al., 2017). In the center of the vesicle, cargo and cargo adapters concentrate as the pit curves. A class of proteins including AP2 inhabits both the edge and center zone and transit between them as vesicles curve. Lastly, a group of proteins bridge the outer zone with the surrounding membrane and likely act as link between vesicles and the actin cortex. Determining this nanoscale organization has allowed for the interactions and mechanistic roles of these proteins to be placed into a local structural context. These data give a dynamic working model of how individual organelles grow and form at the membrane. As CLEM becomes more common, other organelles such as exocytic vesicle, caveolae, the actin cortex, microtubules, and adhesion complexes will similarly gain a curated dynamic molecular structure (Taraska, 2015).

Future directions

Combining the power of multiple imaging modes will allow for a deeper exploration of the structure of the plasma membrane and its associated organelles. While techniques keep improving, it is worth noting that many classic, established, or even underutilized methods can be combined with modern fluorescence techniques to produce incredibly rich images. To accomplish this, pipelines that allow for smooth transitions between techniques that preserve the quality and alignment of the samples between the imaging modes need to be developed (Svitkina and Borisy, 1998; Kukulski et al., 2011; Watanabe et al., 2011; Sochacki et al., 2014; Spiegelhalter et al., 2014; de Boer et al., 2015; Kopek et al., 2017; Paul-Gilloteaux et al., 2017; Peddie et al., 2017). Future work matching dynamic high-resolution live-cell fluorescence with EM and atomic force microscopy should be even more informative. Clearly, the future is bright for exploring the structure of the membrane and its protein landscape.

The plasma membrane was one of the first biological structures to be examined in detail with a resolution that matches its molecular components. The early application of EM to the plasma membrane allowed for the topography of the membrane and its associated structures to be mapped. The plasma membrane's accessibility further facilitated these investigations. Future work localizing the full complement of molecules that drive the biology of the plasma membrane, including lipids, sugars, and all the known and unknown proteins of the system, will provide a dynamic map of how this unique organelle functions in both health and disease. Studying these structures across many different cells, tissues, organisms, and states will reveal the basic fundamental rules of the plasma membrane and how these activities and structures are adapted to the myriad functions of life. Imaging will certainly lead the way toward this ultimate goal.

Acknowledgments

I would like to thank Kem Sochacki, Yael Mutsafi, Bridgette Heine, and Bijeta Prasai for critical reading of the manuscript. I would like to thank Lesley Anson for editorial assistance on the development of the manuscript. Kem Sochacki, Bijeta Prasai, and Regina Ahn produced and provided light microscopy and EM images for this review.

J.W. Taraska is supported by the National Heart, Lung, and Blood Institute, National Institutes of Health (Intramural Research Program).

The author declares no competing interests.

Lesley C. Anson served as editor.

Submitted: 12 April 2019
Accepted: 10 June 2019

References

Anantharam, A., B. Onoa, R.H. Edwards, R.W. Holz, and D. Axelrod. 2010. Localized topological changes of the plasma membrane upon exocytosis visualized by polarized TIRFM. *J. Cell Biol.* 188:415–428. https://doi.org/10.1083/jcb.200908010

Anantharam, A., M.A. Bittner, R.L. Aikman, E.L. Stuenkel, S.L. Schmid, D. Axelrod, and R.W. Holz. 2011. A new role for the dynamin GTPase in the regulation of fusion pore expansion. *Mol. Biol. Cell.* 22:1907–1918. https://doi.org/10.1091/mbc.e11-02-0101

Avery, J., D.J. Ellis, T. Lang, P. Holroyd, D. Riedel, R.M. Henderson, J.M. Edwardson, and R. Jahn. 2000. A cell-free system for regulated exocytosis in PC12 cells. *J. Cell Biol.* 148:317–324. https://doi.org/10.1083/jcb.148.2.317

Avinoam, O., M. Schorb, C.J. Beese, J.A. Briggs, and M. Kaksonen. 2015. Endocytic sites mature by continuous bending and remodeling of the clathrin coat. *Science.* 348:1369–1372. https://doi.org/10.1126/science.aaa9555

Axelrod, D. 1981. Cell-substrate contacts illuminated by total internal reflection fluorescence. *J. Cell Biol.* 89:141–145. https://doi.org/10.1083/jcb.89.1.141

Axelrod, D. 2013. Evanescent excitation and emission in fluorescence microscopy. *Biophys. J.* 104:1401–1409. https://doi.org/10.1016/j.bpj.2013.02.044

Balzarotti, F., Y. Eilers, K.C. Gwosch, A.H. Gynnå, V. Westphal, F.D. Stefani, J. Elf, and S.W. Hell. 2017. Nanometer resolution imaging and tracking of fluorescent molecules with minimal photon fluxes. *Science.* 355:606–612. https://doi.org/10.1126/science.aak9913

Beck, M., and W. Baumeister. 2016. Cryo-Electron Tomography: Can it Reveal the Molecular Sociology of Cells in Atomic Detail? *Trends Cell Biol.* 26:825–837. https://doi.org/10.1016/j.tcb.2016.08.006

Beghin, A., A. Kechkar, C. Butler, F. Levet, M. Cabillic, O. Rossier, G. Giannone, R. Galland, D. Choquet, and J.B. Sibarita. 2017. Localization-based super-resolution imaging meets high-content screening. *Nat. Methods.* 14:1184–1190. https://doi.org/10.1038/nmeth.4486

Betzig, E. 1995. Proposed method for molecular optical imaging. *Opt. Lett.* 20:237–239. https://doi.org/10.1364/OL.20.000237

Betzig, E., G.H. Patterson, R. Sougrat, O.W. Lindwasser, S. Olenych, J.S. Bonifacino, M.W. Davidson, J. Lippincott-Schwartz, and H.F. Hess. 2006. Imaging intracellular fluorescent proteins at nanometer resolution. *Science.* 313:1642–1645. https://doi.org/10.1126/science.1127344

Briggman, K.L., and D.D. Bock. 2012. Volume electron microscopy for neuronal circuit reconstruction. *Curr. Opin. Neurobiol.* 22:154–161. https://doi.org/10.1016/j.conb.2011.10.022

Briggman, K.L., M. Helmstaedter, and W. Denk. 2011. Wiring specificity in the direction-selectivity circuit of the retina. *Nature.* 471:183–188. https://doi.org/10.1038/nature09818

Bykov, Y.S., M. Schaffer, S.O. Dodonova, S. Albert, J.M. Plitzko, W. Baumeister, B.D. Engel, and J.A. Briggs. 2017. The structure of the COPI coat determined within the cell. *eLife.* 6:e32493. https://doi.org/10.7554/eLife.32493

Cabezas, P., and C. Risco. 2006. Studying cellular architecture in three dimensions with improved resolution: Ta replicas revisited. *Cell Biol. Int.* 30:747–754. https://doi.org/10.1016/j.cellbi.2006.05.006

Caicedo, J.C., S. Cooper, F. Heigwer, S. Warchal, P. Qiu, C. Molnar, A.S. Vasilevich, J.D. Barry, H.S. Bansal, O. Kraus, et al. 2017. Data-analysis strategies for image-based cell profiling. *Nat. Methods.* 14:849–863. https://doi.org/10.1038/nmeth.4397

Chang, Y.W., S. Chen, E.I. Tocheva, A. Treuner-Lange, S. Löbach, L. Søgaard-Andersen, and G.J. Jensen. 2014. Correlated cryogenic photoactivated localization microscopy and cryo-electron tomography. *Nat. Methods.* 11:737–739. https://doi.org/10.1038/nmeth.2961

Cheng, Y. 2018. Single-particle cryo-EM-How did it get here and where will it go. *Science.* 361:876–880. https://doi.org/10.1126/science.aat4346

Clarke, M., G. Schatten, D. Mazia, and J.A. Spudich. 1975. Visualization of actin fibers associated with the cell membrane in amoebae of Dictyostelium discoideum. *Proc. Natl. Acad. Sci. USA.* 72:1758–1762. https://doi.org/10.1073/pnas.72.5.1758

Collins, A., A. Warrington, K.A. Taylor, and T. Svitkina. 2011. Structural organization of the actin cytoskeleton at sites of clathrin-mediated endocytosis. *Curr. Biol.* 21:1167–1175. https://doi.org/10.1016/j.cub.2011.05.048

Coltharp, C., X. Yang, and J. Xiao. 2014. Quantitative analysis of single-molecule superresolution images. *Curr. Opin. Struct. Biol.* 28:112–121. https://doi.org/10.1016/j.sbi.2014.08.008

Crivat, G., and J.W. Taraska. 2012. Imaging proteins inside cells with fluorescent tags. *Trends Biotechnol.* 30:8–16. https://doi.org/10.1016/j.tibtech.2011.08.002

Danielli, J.F. 1935. The Thickness of the Wall of the Red Blood Corpuscle. *J. Gen. Physiol.* 19:19–22. https://doi.org/10.1085/jgp.19.1.19

de Boer, P., J.P. Hoogenboom, and B.N. Giepmans. 2015. Correlated light and electron microscopy: ultrastructure lights up! *Nat. Methods.* 12:503–513. https://doi.org/10.1038/nmeth.3400

de Chaumont, F., S. Dallongeville, N. Chenouard, N. Hervé, S. Pop, T. Provoost, V. Meas-Yedid, P. Pankajakshan, T. Lecomte, Y. Le Montagner, et al. 2012. Icy: an open bioimage informatics platform for extended reproducible research. *Nat. Methods.* 9:690–696. https://doi.org/10.1038/nmeth.2075

Egner, A., and S.W. Hell. 2005. Fluorescence microscopy with super-resolved optical sections. *Trends Cell Biol.* 15:207–215. https://doi.org/10.1016/j.tcb.2005.02.003

Eliceiri, K.W., M.R. Berthold, I.G. Goldberg, L. Ibáñez, B.S. Manjunath, M.E. Martone, R.F. Murphy, H. Peng, A.L. Plant, B. Roysam, et al. 2012. Biological imaging software tools. *Nat. Methods.* 9:697–710. https://doi.org/10.1038/nmeth.2084

Engel, B.D., M. Schaffer, S. Albert, S. Asano, J.M. Plitzko, and W. Baumeister. 2015. In situ structural analysis of Golgi intracisternal protein arrays. *Proc. Natl. Acad. Sci. USA.* 112:11264–11269. https://doi.org/10.1073/pnas.1515337112

Fricke, H. 1925. The Electric Capacity of Suspensions with Special Reference to Blood. *J. Gen. Physiol.* 9:137–152. https://doi.org/10.1085/jgp.9.2.137

Fricke, H., and S. Morse. 1925. The Electric Resistance and Capacity of Blood for Frequencies between 800 and 4|Million Cycles. *J. Gen. Physiol.* 9:153–167. https://doi.org/10.1085/jgp.9.2.153

Funatsu, T., Y. Harada, M. Tokunaga, K. Saito, and T. Yanagida. 1995. Imaging of single fluorescent molecules and individual ATP turnovers by single

myosin molecules in aqueous solution. *Nature.* 374:555–559. https://doi.org/10.1038/374555a0

Gan, L., and G.J. Jensen. 2012. Electron tomography of cells. *Q. Rev. Biophys.* 45:27–56. https://doi.org/10.1017/S0033583511000102

Glaeser, R.M. 2013. Invited review article: Methods for imaging weak-phase objects in electron microscopy. *Rev. Sci. Instrum.* 84:111101. https://doi.org/10.1063/1.4830355

Glancy, B., L.M. Hartnell, D. Malide, Z.X. Yu, C.A. Combs, P.S. Connelly, S. Subramaniam, and R.S. Balaban. 2015. Mitochondrial reticulum for cellular energy distribution in muscle. *Nature.* 523:617–620. https://doi.org/10.1038/nature14614

Glauert, A.M., and R.H. Glauert. 1958. Araldite as an embedding medium for electron microscopy. *J. Biophys. Biochem. Cytol.* 4:191–194. https://doi.org/10.1083/jcb.4.2.191

Glauert, A.M., R.H. Glauert, and G.E. Rogers. 1956. A new embedding medium for electron microscopy. *Nature.* 178:803. https://doi.org/10.1038/178803a0

Gorter, E., and F. Grendel. 1925. On Bimolecular Layers of Lipoids on the Chromocytes of the Blood. *J. Exp. Med.* 41:439–443. https://doi.org/10.1084/jem.41.4.439

Graffe, M., D. Zenisek, and J.W. Taraska. 2015. A marginal band of microtubules transports and organizes mitochondria in retinal bipolar synaptic terminals. *J. Gen. Physiol.* 146:109–117. https://doi.org/10.1085/jgp.201511396

Guo, M., P. Chandris, J.P. Giannini, A.J. Trexler, R. Fischer, J. Chen, H.D. Vishwasrao, I. Rey-Suarez, Y. Wu, X. Wu, et al. 2018. Single-shot super-resolution total internal reflection fluorescence microscopy. *Nat. Methods.* 15:425–428. https://doi.org/10.1038/s41592-018-0004-4

Gustafsson, M.G. 2000. Surpassing the lateral resolution limit by a factor of two using structured illumination microscopy. *J. Microsc.* 198:82–87. https://doi.org/10.1046/j.1365-2818.2000.00710.x

Hall, C.E., M.A. Jakus, and F.O. Schmitt. 1945. The Structure of Certain Muscle Fibrils as Revealed by the Use of Electron Stains. *J. Appl. Phys.* 16:459–465. https://doi.org/10.1063/1.1707615

Hanson, P.I., R. Roth, Y. Lin, and J.E. Heuser. 2008. Plasma membrane deformation by circular arrays of ESCRT-III protein filaments. *J. Cell Biol.* 180:389–402. https://doi.org/10.1083/jcb.200707031

Harris, K.M., E. Perry, J. Bourne, M. Feinberg, L. Ostroff, and J. Hurlburt. 2006. Uniform serial sectioning for transmission electron microscopy. *J. Neurosci.* 26:12101–12103. https://doi.org/10.1523/JNEUROSCI.3994-06.2006

Haucke, V., and M.M. Kozlov. 2018. Membrane remodeling in clathrin-mediated endocytosis. *J. Cell Sci.* 131:jcs216812. https://doi.org/10.1242/jcs.216812

Hauser, M., M. Wojcik, D. Kim, M. Mahmoudi, W. Li, and K. Xu. 2017. Correlative Super-Resolution Microscopy: New Dimensions and New Opportunities. *Chem. Rev.* 117:7428–7456. https://doi.org/10.1021/acs.chemrev.6b00604

Hell, S.W., and J. Wichmann. 1994. Breaking the diffraction resolution limit by stimulated emission: stimulated-emission-depletion fluorescence microscopy. *Opt. Lett.* 19:780–782. https://doi.org/10.1364/OL.19.000780

Helmstaedter, M., K.L. Briggman, S.C. Turaga, V. Jain, H.S. Seung, and W. Denk. 2013. Connectomic reconstruction of the inner plexiform layer in the mouse retina. *Nature.* 500:168–174. https://doi.org/10.1038/nature12346

Henderson, R. 2015. Overview and future of single particle electron cryomicroscopy. *Arch. Biochem. Biophys.* 581:19–24. https://doi.org/10.1016/j.abb.2015.02.036

Hess, S.T., T.P. Girirajan, and M.D. Mason. 2006. Ultra-high resolution imaging by fluorescence photoactivation localization microscopy. *Biophys. J.* 91:4258–4272. https://doi.org/10.1529/biophysj.106.091116

Heuser, J. 1980. Three-dimensional visualization of coated vesicle formation in fibroblasts. *J. Cell Biol.* 84:560–583. https://doi.org/10.1083/jcb.84.3.560

Heuser, J.E. 1986. Different structural states of a microtubule cross-linking molecule, captured by quick-freezing motile axostyles in protozoa. *J. Cell Biol.* 103:2209–2227. https://doi.org/10.1083/jcb.103.6.2209

Heuser, J. 1989. Effects of cytoplasmic acidification on clathrin lattice morphology. *J. Cell Biol.* 108:401–411. https://doi.org/10.1083/jcb.108.2.401

Heuser, J. 2000. The production of 'cell cortices' for light and electron microscopy. *Traffic.* 1:545–552. https://doi.org/10.1034/j.1600-0854.2000.010704.x

Heuser, J.E. 2014. Some personal and historical notes on the utility of "deep-etch" electron microscopy for making cell structure/function correlations. *Mol. Biol. Cell.* 25:3273–3276. https://doi.org/10.1091/mbc.e14-05-1016

Heuser, J.E., and J. Keen. 1988. Deep-etch visualization of proteins involved in clathrin assembly. *J. Cell Biol.* 107:877–886. https://doi.org/10.1083/jcb.107.3.877

Heuser, J.E., and M.W. Kirschner. 1980. Filament organization revealed in platinum replicas of freeze-dried cytoskeletons. *J. Cell Biol.* 86:212–234. https://doi.org/10.1083/jcb.86.1.212

Heuser, J.E., and T.S. Reese. 1981. Structural changes after transmitter release at the frog neuromuscular junction. *J. Cell Biol.* 88:564–580. https://doi.org/10.1083/jcb.88.3.564

Heuser, J.E., and S.R. Salpeter. 1979. Organization of acetylcholine receptors in quick-frozen, deep-etched, and rotary-replicated Torpedo postsynaptic membrane. *J. Cell Biol.* 82:150–173. https://doi.org/10.1083/jcb.82.1.150

Hooke, R. 1665. *Micrographia: or, Some physiological descriptions of minute bodies made by magnifying glasses. With observations and inquiries thereupon.* J. Martyn and J. Allestry, London. https://doi.org/10.5962/bhl.title.105738

Huang, B., M. Bates, and X. Zhuang. 2009. Super-resolution fluorescence microscopy. *Annu. Rev. Biochem.* 78:993–1016. https://doi.org/10.1146/annurev.biochem.77.061906.092014

Huang, B., H. Babcock, and X. Zhuang. 2010. Breaking the diffraction barrier: super-resolution imaging of cells. *Cell.* 143:1047–1058. https://doi.org/10.1016/j.cell.2010.12.002

Ishikawa, H., J. Usukura, and E. Yamada. 1982. Application of cryomicrotomy to the rapid-freeze, deep-etch replica method for unfixed tissues and cells. *J. Electron Microsc. (Tokyo).* 31:198–201.

Jacobson, K., P. Liu, and B.C. Lagerholm. 2019. The Lateral Organization and Mobility of Plasma Membrane Components. *Cell.* 177:806–819. https://doi.org/10.1016/j.cell.2019.04.018

Ji, N., H. Shroff, H. Zhong, and E. Betzig. 2008. Advances in the speed and resolution of light microscopy. *Curr. Opin. Neurobiol.* 18:605–616. https://doi.org/10.1016/j.conb.2009.03.009

Jordan, M.A., D.R. Diener, L. Stepanek, and G. Pigino. 2018. The cryo-EM structure of intraflagellar transport trains reveals how dynein is inactivated to ensure unidirectional anterograde movement in cilia. *Nat. Cell Biol.* 20:1250–1255. https://doi.org/10.1038/s41556-018-0213-1

Kanchanawong, P., G. Shtengel, A.M. Pasapera, E.B. Ramko, M.W. Davidson, H.F. Hess, and C.M. Waterman. 2010. Nanoscale architecture of integrin-based cell adhesions. *Nature.* 468:580–584. https://doi.org/10.1038/nature09621

Karreman, M.A., V. Hyenne, Y. Schwab, and J.G. Goetz. 2016. Intravital Correlative Microscopy: Imaging Life at the Nanoscale. *Trends Cell Biol.* 26:848–863. https://doi.org/10.1016/j.tcb.2016.07.003

Kizilyaprak, C., Y.D. Stierhof, and B.M. Humbel. 2018. Volume microscopy in biology: FIB-SEM tomography. *Tissue Cell.* 57:123–128.

Kner, P., B.B. Chhun, E.R. Griffis, L. Winoto, and M.G. Gustafsson. 2009. Super-resolution video microscopy of live cells by structured illumination. *Nat. Methods.* 6:339–342. https://doi.org/10.1038/nmeth.1324

Kopek, B.G., G. Shtengel, J.B. Grimm, D.A. Clayton, and H.F. Hess. 2013. Correlative photoactivated localization and scanning electron microscopy. *PLoS One.* 8:e77209. https://doi.org/10.1371/journal.pone.0077209

Kopek, B.G., M.G. Paez-Segala, G. Shtengel, K.A. Sochacki, M.G. Sun, Y. Wang, C.S. Xu, S.B. van Engelenburg, J.W. Taraska, L.L. Looger, and H.F. Hess. 2017. Diverse protocols for correlative super-resolution fluorescence imaging and electron microscopy of chemically fixed samples. *Nat. Protoc.* 12:916–946. https://doi.org/10.1038/nprot.2017.017

Kovtun, O., N. Leneva, Y.S. Bykov, N. Ariotti, R.D. Teasdale, M. Schaffer, B.D. Engel, D.J. Owen, J.A.G. Briggs, and B.M. Collins. 2018. Structure of the membrane-assembled retromer coat determined by cryo-electron tomography. *Nature.* 561:561–564. https://doi.org/10.1038/s41586-018-0526-z

Krystofiak, E.S., J.B. Heymann, and B. Kachar. 2019. Carbon replicas reveal double stranded structure of tight junctions in phase-contrast electron microscopy. *Commun Biol.* 2:98. https://doi.org/10.1038/s42003-019-0319-4

Kukulski, W., M. Schorb, S. Welsch, A. Picco, M. Kaksonen, and J.A. Briggs. 2011. Correlated fluorescence and 3D electron microscopy with high sensitivity and spatial precision. *J. Cell Biol.* 192:111–119. https://doi.org/10.1083/jcb.201009037

Kukulski, W., M. Schorb, M. Kaksonen, and J.A. Briggs. 2012. Plasma membrane reshaping during endocytosis is revealed by time-resolved electron tomography. *Cell.* 150:508–520. https://doi.org/10.1016/j.cell.2012.05.046

Kukulski, W., A. Picco, T. Specht, J.A. Briggs, and M. Kaksonen. 2016. Clathrin modulates vesicle scission, but not invagination shape, in yeast endocytosis. *eLife.* 5:e16036. https://doi.org/10.7554/eLife.16036

Kusumi, A., T.K. Fujiwara, R. Chadda, M. Xie, T.A. Tsunoyama, Z. Kalay, R.S. Kasai, and K.G. Suzuki. 2012. Dynamic organizing principles of the plasma membrane that regulate signal transduction: commemorating the fortieth anniversary of Singer and Nicolson's fluid-mosaic model. *Annu. Rev. Cell Dev. Biol.* 28:215–250. https://doi.org/10.1146/annurev-cellbio-100809-151736

Larson, B.T., K.A. Sochacki, J.M. Kindem, and J.W. Taraska. 2014. Systematic spatial mapping of proteins at exocytic and endocytic structures. *Mol. Biol. Cell.* 25:2084–2093. https://doi.org/10.1091/mbc.e14-02-0771

Leterrier, C., P. Dubey, and S. Roy. 2017. The nano-architecture of the axonal cytoskeleton. *Nat. Rev. Neurosci.* 18:713–726. https://doi.org/10.1038/nrn.2017.129

Levet, F., E. Hosy, A. Kechkar, C. Butler, A. Beghin, D. Choquet, and J.B. Sibarita. 2015. SR-Tesseler: a method to segment and quantify localization-based super-resolution microscopy data. *Nat. Methods.* 12:1065–1071. https://doi.org/10.1038/nmeth.3579

Loussert Fonta, C., and B.M. Humbel. 2015. Correlative microscopy. *Arch. Biochem. Biophys.* 581:98–110. https://doi.org/10.1016/j.abb.2015.05.017

Mahamid, J., S. Pfeffer, M. Schaffer, E. Villa, R. Danev, L.K. Cuellar, F. Förster, A.A. Hyman, J.M. Plitzko, and W. Baumeister. 2016. Visualizing the molecular sociology at the HeLa cell nuclear periphery. *Science.* 351:969–972. https://doi.org/10.1126/science.aad8857

Manley, S., J.M. Gillette, G.H. Patterson, H. Shroff, H.F. Hess, E. Betzig, and J. Lippincott-Schwartz. 2008. High-density mapping of single-molecule trajectories with photoactivated localization microscopy. *Nat. Methods.* 5:155–157. https://doi.org/10.1038/nmeth.1176

Mastronarde, D.N., and S.R. Held. 2017. Automated tilt series alignment and tomographic reconstruction in IMOD. *J. Struct. Biol.* 197:102–113. https://doi.org/10.1016/j.jsb.2016.07.011

Mattheyses, A.L., S.M. Simon, and J.Z. Rappoport. 2010. Imaging with total internal reflection fluorescence microscopy for the cell biologist. *J. Cell Sci.* 123:3621–3628. https://doi.org/10.1242/jcs.056218

Mazia, D., G. Schatten, and W. Sale. 1975. Adhesion of cells to surfaces coated with polylysine. Applications to electron microscopy. *J. Cell Biol.* 66:198–200. https://doi.org/10.1083/jcb.66.1.198

Meier, C., and A. Beckmann. 2018. Freeze fracture: new avenues for the ultrastructural analysis of cells in vitro. *Histochem. Cell Biol.* 149:3–13. https://doi.org/10.1007/s00418-017-1617-x

Milne, J.L., M.J. Borgnia, A. Bartesaghi, E.E. Tran, L.A. Earl, D.M. Schauder, J. Lengyel, J. Pierson, A. Patwardhan, and S. Subramaniam. 2013. Cryo-electron microscopy--a primer for the non-microscopist. *FEBS J.* 280:28–45. https://doi.org/10.1111/febs.12078

Moberg, C.L. 1995. The electron microscope enters the realm of the intact cell. *J. Exp. Med.* 181:831–837. https://doi.org/10.1084/jem.181.3.831

Moen, E., D. Bannon, T. Kudo, W. Graf, M. Covert, and D. Van Valen. 2019. Deep learning for cellular image analysis. *Nat. Methods.* https://doi.org/10.1038/s41592-019-0403-1

Morone, N., T. Fujiwara, K. Murase, R.S. Kasai, H. Ike, S. Yuasa, J. Usukura, and A. Kusumi. 2006. Three-dimensional reconstruction of the membrane skeleton at the plasma membrane interface by electron tomography. *J. Cell Biol.* 174:851–862. https://doi.org/10.1083/jcb.200606007

Mund, M., J.A. van der Beek, J. Deschamps, S. Dmitrieff, P. Hoess, J.L. Monster, A. Picco, F. Nedelec, M. Kaksonen, and J. Ries. 2018. Systematic Nanoscale Analysis of Endocytosis Links Efficient Vesicle Formation to Patterned Actin Nucleation. *Cell.* 174:884–896.

Myers, G. 2012. Why bioimage informatics matters. *Nat. Methods.* 9:659–660. https://doi.org/10.1038/nmeth.2024

Nickell, S., C. Kofler, A.P. Leis, and W. Baumeister. 2006. A visual approach to proteomics. *Nat. Rev. Mol. Cell Biol.* 7:225–230. https://doi.org/10.1038/nrm1861

Ognjenović, J., R. Grisshammer, and S. Subramaniam. 2019. Frontiers in Cryo Electron Microscopy of Complex Macromolecular Assemblies. *Annu. Rev. Biomed. Eng.* 21:395–415. https://doi.org/10.1146/annurev-bioeng-060418-052453

Oikonomou, C.M., and G.J. Jensen. 2017. Cellular Electron Cryotomography: Toward Structural Biology In Situ. *Annu. Rev. Biochem.* 86:873–896. https://doi.org/10.1146/annurev-biochem-061516-044741

Olveczky, B.P., N. Periasamy, and A.S. Verkman. 1997. Mapping fluorophore distributions in three dimensions by quantitative multiple angle-total internal reflection fluorescence microscopy. *Biophys. J.* 73:2836–2847. https://doi.org/10.1016/S0006-3495(97)78312-7

Passmore, D.R., T. Rao, and A. Anantharam. 2014. Real-time investigation of plasma membrane deformation and fusion pore expansion using polarized Total Internal Reflection Fluorescence Microscopy. *Methods Mol. Biol.* 1174:263–273. https://doi.org/10.1007/978-1-4939-0944-5_18

Patterson, G.H., and J. Lippincott-Schwartz. 2002. A photoactivatable GFP for selective photolabeling of proteins and cells. *Science.* 297:1873–1877. https://doi.org/10.1126/science.1074952

Patterson, G., M. Davidson, S. Manley, and J. Lippincott-Schwartz. 2010. Superresolution imaging using single-molecule localization. *Annu. Rev. Phys. Chem.* 61:345–367. https://doi.org/10.1146/annurev.physchem.012809.103444

Paul-Gilloteaux, P., X. Heiligenstein, M. Belle, M.C. Domart, B. Larijani, L. Collinson, G. Raposo, and J. Salamero. 2017. eC-CLEM: flexible multidimensional registration software for correlative microscopies. *Nat. Methods.* 14:102–103. https://doi.org/10.1038/nmeth.4170

Peddie, C.J., M.C. Domart, X. Snetkov, P. O'Toole, B. Larijani, M. Way, S. Cox, and L.M. Collinson. 2017. Correlative super-resolution fluorescence and electron microscopy using conventional fluorescent proteins in vacuo. *J. Struct. Biol.* 199:120–131. https://doi.org/10.1016/j.jsb.2017.05.013

Penn, A.C., C.L. Zhang, F. Georges, L. Royer, C. Breillat, E. Hosy, J.D. Petersen, Y. Humeau, and D. Choquet. 2017. Hippocampal LTP and contextual learning require surface diffusion of AMPA receptors. *Nature.* 549:384–388. https://doi.org/10.1038/nature23658

Picco, A., M. Mund, J. Ries, F. Nédélec, and M. Kaksonen. 2015. Visualizing the functional architecture of the endocytic machinery. *eLife.* 4:e04535. https://doi.org/10.7554/eLife.04535

Porter, K.R., and J. Blum. 1953. A study in microtomy for electron microscopy. *Anat. Rec.* 117:685–710. https://doi.org/10.1002/ar.1091170403

Porter, K.R., A. Claude, and E.F. Fullam. 1945. A Study of Tissue Culture Cells by Electron Microscopy: Methods and Preliminary Observations. *J. Exp. Med.* 81:233–246. https://doi.org/10.1084/jem.81.3.233

Robertson, J.D. 1981. Membrane structure. *J. Cell Biol.* 91:189s–204s. https://doi.org/10.1083/jcb.91.3.189s

Robertson, J.L. 2018. The lipid bilayer membrane and its protein constituents. *J. Gen. Physiol.* 150:1472–1483. https://doi.org/10.1085/jgp.201812153

Rohrbach, A. 2000. Observing secretory granules with a multiangle evanescent wave microscope. *Biophys. J.* 78:2641–2654. https://doi.org/10.1016/S0006-3495(00)76808-1

Roth, T.F., and K.R. Porter. 1964. Yolk Protein Uptake in the Oocyte of the Mosquito Aedes Aegypti. L. *J. Cell Biol.* 20:313–332. https://doi.org/10.1083/jcb.20.2.313

Rothberg, K.G., J.E. Heuser, W.C. Donzell, Y.S. Ying, J.R. Glenney, and R.G. Anderson. 1992. Caveolin, a protein component of caveolae membrane coats. *Cell.* 68:673–682. https://doi.org/10.1016/0092-8674(92)90143-Z

Russell, M.R., T.R. Lerner, J.J. Burden, D.O. Nkwe, A. Pelchen-Matthews, M.C. Domart, J. Durgan, A. Weston, M.L. Jones, C.J. Peddie, et al. 2017. 3D correlative light and electron microscopy of cultured cells using serial blockface scanning electron microscopy. *J. Cell Sci.* 130:278–291. https://doi.org/10.1242/jcs.188433

Rust, M.J., M. Bates, and X. Zhuang. 2006. Sub-diffraction-limit imaging by stochastic optical reconstruction microscopy (STORM). *Nat. Methods.* 3:793–795. https://doi.org/10.1038/nmeth929

Satir, P. 1997. Keith R. Porter and the first electron micrograph of a cell. *Endeavour.* 21:169–171. https://doi.org/10.1016/S0160-9327(97)01084-3

Schindelin, J., I. Arganda-Carreras, E. Frise, V. Kaynig, M. Longair, T. Pietzsch, S. Preibisch, C. Rueden, S. Saalfeld, B. Schmid, et al. 2012. Fiji: an open-source platform for biological-image analysis. *Nat. Methods.* 9:676–682. https://doi.org/10.1038/nmeth.2019

Schorb, M., I. Haberbosch, W.J.H. Hagen, Y. Schwab, and D.N. Mastronarde. 2019. Software tools for automated transmission electron microscopy. *Nat. Methods.* 16:471–477. https://doi.org/10.1038/s41592-019-0396-9

Schur, F.K., W.J. Hagen, A. de Marco, and J.A. Briggs. 2013. Determination of protein structure at 8.5Å resolution using cryo-electron tomography and sub-tomogram averaging. *J. Struct. Biol.* 184:394–400. https://doi.org/10.1016/j.jsb.2013.10.015

Scott, B.L., K.A. Sochacki, S.T. Low-Nam, E.M. Bailey, Q. Luu, A. Hor, A.M. Dickey, S. Smith, J.G. Kerkvliet, J.W. Taraska, and A.D. Hoppe. 2018. Membrane bending occurs at all stages of clathrin-coat assembly and defines endocytic dynamics. *Nat. Commun.* 9:419. https://doi.org/10.1038/s41467-018-02818-8

Shin, W., L. Ge, G. Arpino, S.A. Villarreal, E. Hamid, H. Liu, W.D. Zhao, P.J. Wen, H.C. Chiang, and L.G. Wu. 2018. Visualization of Membrane Pore in Live Cells Reveals a Dynamic-Pore Theory Governing Fusion and Endocytosis. *Cell.* 173:934–945.

Sigal, Y.M., R. Zhou, and X. Zhuang. 2018. Visualizing and discovering cellular structures with super-resolution microscopy. *Science.* 361:880–887. https://doi.org/10.1126/science.aau1044

Singer, S.J. 1974. The molecular organization of membranes. *Annu. Rev. Biochem.* 43:805–833. https://doi.org/10.1146/annurev.bi.43.070174.004105

Singer, S.J., and G.L. Nicolson. 1972. The fluid mosaic model of the structure of cell membranes. *Science.* 175:720–731. https://doi.org/10.1126/science.175.4023.720

Sochacki, K.A., and J.W. Taraska. 2017. Correlative Fluorescence Super-Resolution Localization Microscopy and Platinum Replica EM on Unroofed Cells. *Methods Mol. Biol.* 1663:219–230. https://doi.org/10.1007/978-1-4939-7265-4_18

Sochacki, K.A., and J.W. Taraska. 2019. From Flat to Curved Clathrin: Controlling a Plastic Ratchet. *Trends Cell Biol.* 29:241–256. https://doi.org/10.1016/j.tcb.2018.12.002

Sochacki, K.A., B.T. Larson, D.C. Sengupta, M.P. Daniels, G. Shtengel, H.F. Hess, and J.W. Taraska. 2012. Imaging the post-fusion release and capture of a vesicle membrane protein. *Nat. Commun.* 3:1154. https://doi.org/10.1038/ncomms2158

Sochacki, K.A., G. Shtengel, S.B. van Engelenburg, H.F. Hess, and J.W. Taraska. 2014. Correlative super-resolution fluorescence and metal-replica transmission electron microscopy. *Nat. Methods.* 11:305–308. https://doi.org/10.1038/nmeth.2816

Sochacki, K.A., A.M. Dickey, M.P. Strub, and J.W. Taraska. 2017. Endocytic proteins are partitioned at the edge of the clathrin lattice in mammalian cells. *Nat. Cell Biol.* 19:352–361. https://doi.org/10.1038/ncb3498

Specht, E.A., E. Braselmann, and A.E. Palmer. 2017. A Critical and Comparative Review of Fluorescent Tools for Live-Cell Imaging. *Annu. Rev. Physiol.* 79:93–117. https://doi.org/10.1146/annurev-physiol-022516-034055

Spiegelhalter, C., J.F. Laporte, and Y. Schwab. 2014. Correlative light and electron microscopy: from live cell dynamic to 3D ultrastructure. *Methods Mol. Biol.* 1117:485–501. https://doi.org/10.1007/978-1-62703-776-1_21

Steyer, J.A., and W. Almers. 2001. A real-time view of life within 100 nm of the plasma membrane. *Nat. Rev. Mol. Cell Biol.* 2:268–275. https://doi.org/10.1038/35067069

Stone, M.B., S.A. Shelby, M.F. Núñez, K. Wisser, and S.L. Veatch. 2017. Protein sorting by lipid phase-like domains supports emergent signaling function in B lymphocyte plasma membranes. *eLife.* 6:e19891. https://doi.org/10.7554/eLife.19891

Sund, S.E., J.A. Swanson, and D. Axelrod. 1999. Cell membrane orientation visualized by polarized total internal reflection fluorescence. *Biophys. J.* 77:2266–2283. https://doi.org/10.1016/S0006-3495(99)77066-9

Svitkina, T.M., and G.G. Borisy. 1998. Correlative light and electron microscopy of the cytoskeleton of cultured cells. *Methods Enzymol.* 298:570–592. https://doi.org/10.1016/S0076-6879(98)98045-4

Svitkina, T.M., and G.G. Borisy. 1999. Arp2/3 complex and actin depolymerizing factor/cofilin in dendritic organization and treadmilling of actin filament array in lamellipodia. *J. Cell Biol.* 145:1009–1026. https://doi.org/10.1083/jcb.145.5.1009

Svitkina, T.M., A.A. Neyfakh Jr., and A.D. Bershadsky. 1986. Actin cytoskeleton of spread fibroblasts appears to assemble at the cell edges. *J. Cell Sci.* 82:235–248.

Taraska, J.W. 2015. Cell biology of the future: Nanometer-scale cellular cartography. *J. Cell Biol.* 211:211–214. https://doi.org/10.1083/jcb.201508021

Taraska, J.W., and W. Almers. 2004. Bilayers merge even when exocytosis is transient. *Proc. Natl. Acad. Sci. USA.* 101:8780–8785. https://doi.org/10.1073/pnas.0401316101

Taraska, J.W., and W.N. Zagotta. 2010. Fluorescence applications in molecular neurobiology. *Neuron.* 66:170–189. https://doi.org/10.1016/j.neuron.2010.02.002

Thompson, R.E., D.R. Larson, and W.W. Webb. 2002. Precise nanometer localization analysis for individual fluorescent probes. *Biophys. J.* 82:2775–2783. https://doi.org/10.1016/S0006-3495(02)75618-X

Tsukita, S., J. Usukura, S. Tsukita, and H. Ishikawa. 1982. The cytoskeleton in myelinated axons: a freeze-etch replica study. *Neuroscience.* 7:2135–2147. https://doi.org/10.1016/0306-4522(82)90125-7

Vacquier, V.D. 1975. The isolation of intact cortical granules from sea urchin eggs: calcium lons trigger granule discharge. *Dev. Biol.* 43:62–74. https://doi.org/10.1016/0012-1606(75)90131-1

Vassilopoulos, S., C. Gentil, J. Lainé, P.O. Buclez, A. Franck, A. Ferry, G. Précigout, R. Roth, J.E. Heuser, F.M. Brodsky, et al. 2014. Actin scaffolding by clathrin heavy chain is required for skeletal muscle sarcomere organization. *J. Cell Biol.* 205:377–393. https://doi.org/10.1083/jcb.201309096

Villa, E., and K. Lasker. 2014. Finding the right fit: chiseling structures out of cryo-electron microscopy maps. *Curr. Opin. Struct. Biol.* 25:118–125. https://doi.org/10.1016/j.sbi.2014.04.001

Villa, E., M. Schaffer, J.M. Plitzko, and W. Baumeister. 2013. Opening windows into the cell: focused-ion-beam milling for cryo-electron tomography. *Curr. Opin. Struct. Biol.* 23:771–777. https://doi.org/10.1016/j.sbi.2013.08.006

Walter, T., D.W. Shattuck, R. Baldock, M.E. Bastin, A.E. Carpenter, S. Duce, J. Ellenberg, A. Fraser, N. Hamilton, S. Pieper, et al. 2010. Visualization of image data from cells to organisms. *Nat. Methods.* 7(3 Suppl):S26–S41. https://doi.org/10.1038/nmeth.1431

Wan, W., and J.A. Briggs. 2016. Cryo-Electron Tomography and Subtomogram Averaging. *Methods Enzymol.* 579:329–367. https://doi.org/10.1016/bs.mie.2016.04.014

Watanabe, S., A. Punge, G. Hollopeter, K.I. Willig, R.J. Hobson, M.W. Davis, S.W. Hell, and E.M. Jorgensen. 2011. Protein localization in electron micrographs using fluorescence nanoscopy. *Nat. Methods.* 8:80–84. https://doi.org/10.1038/nmeth.1537

Watson, M.L. 1958a. Staining of tissue sections for electron microscopy with heavy metals. *J. Biophys. Biochem. Cytol.* 4:475–478. https://doi.org/10.1083/jcb.4.4.475

Watson, M.L. 1958b. Staining of tissue sections for electron microscopy with heavy metals. II. Application of solutions containing lead and barium. *J. Biophys. Biochem. Cytol.* 4:727–730. https://doi.org/10.1083/jcb.4.6.727

Weigert, M., U. Schmidt, T. Boothe, A. Müller, A. Dibrov, A. Jain, B. Wilhelm, D. Schmidt, C. Broaddus, S. Culley, et al. 2018. Content-aware image restoration: pushing the limits of fluorescence microscopy. *Nat. Methods.* 15:1090–1097. https://doi.org/10.1038/s41592-018-0216-7

Williams, R.C., and R.W. Wyckoff. 1945a. Electron Shadow Micrography of the Tobacco Mosaic Virus Protein. *Science.* 101:594–596. https://doi.org/10.1126/science.101.2632.594

Williams, R.C., and R.W.G. Wyckoff. 1945b. Electron Shadow-Micrographs of Haemocyanin Molecules. *Nature.* 156:68–70. https://doi.org/10.1038/156068a0

Williams, R.C., and R.W.G. Wyckoff. 1946. Metal Shadowing of Preparations for Electron Micrography. *J. Appl. Phys.* 17:67–67.

Winter, P.W., and H. Shroff. 2014. Faster fluorescence microscopy: advances in high speed biological imaging. *Curr. Opin. Chem. Biol.* 20:46–53. https://doi.org/10.1016/j.cbpa.2014.04.008

Wu, Y., and H. Shroff. 2018. Faster, sharper, and deeper: structured illumination microscopy for biological imaging. *Nat. Methods.* 15:1011–1019. https://doi.org/10.1038/s41592-018-0211-z

Wysocki, L.M., and L.D. Lavis. 2011. Advances in the chemistry of small molecule fluorescent probes. *Curr. Opin. Chem. Biol.* 15:752–759. https://doi.org/10.1016/j.cbpa.2011.10.013

Xu, K., G. Zhong, and X. Zhuang. 2013. Actin, spectrin, and associated proteins form a periodic cytoskeletal structure in axons. *Science.* 339:452–456. https://doi.org/10.1126/science.1232251

Xu, M., J. Singla, E.I. Tocheva, Y.W. Chang, R.C. Stevens, G.J. Jensen, and F. Alber. 2019. De Novo Structural Pattern Mining in Cellular Electron Cryotomograms. *Structure.* 27:679–691.e14. https://doi.org/10.1016/j.str.2019.01.005

Yang, C., and T. Svitkina. 2011. Visualizing branched actin filaments in lamellipodia by electron tomography. *Nat. Cell Biol.* 13:1012–1013, author reply:1013–1014. https://doi.org/10.1038/ncb2321

Yang, C., and T.M. Svitkina. 2019. Ultrastructure and dynamics of the actin-myosin II cytoskeleton during mitochondrial fission. *Nat. Cell Biol.* 21:603–613. https://doi.org/10.1038/s41556-019-0313-6

Yildiz, A., J.N. Forkey, S.A. McKinney, T. Ha, Y.E. Goldman, and P.R. Selvin. 2003. Myosin V walks hand-over-hand: single fluorophore imaging with 1.5-nm localization. *Science.* 300:2061–2065. https://doi.org/10.1126/science.1084398

Yildiz, A., M. Tomishige, R.D. Vale, and P.R. Selvin. 2004. Kinesin walks hand-over-hand. *Science.* 303:676–678. https://doi.org/10.1126/science.1093753

Zenisek, D., J.A. Steyer, and W. Almers. 2000. Transport, capture and exocytosis of single synaptic vesicles at active zones. *Nature.* 406:849–854. https://doi.org/10.1038/35022500

Zenisek, D., J.A. Steyer, M.E. Feldman, and W. Almers. 2002. A membrane marker leaves synaptic vesicles in milliseconds after exocytosis in retinal bipolar cells. *Neuron.* 35:1085–1097. https://doi.org/10.1016/S0896-6273(02)00896-6

Zhao, W.D., E. Hamid, W. Shin, P.J. Wen, E.S. Krystofiak, S.A. Villarreal, H.C. Chiang, B. Kachar, and L.G. Wu. 2016. Hemi-fused structure mediates and controls fusion and fission in live cells. *Nature.* 534:548–552. https://doi.org/10.1038/nature18598